Bull. Inst. Chem. Res., Kyoto Univ., Vol. 72, No. 5-6, 1995

Effects of Thermodynamic Confinements on Block Copolymer Dynamics

Hiroshi WATANABE*

Received November 8, 1994

Rheological properties were examined for styrene-butadiene (PS-PB) diblock copolymers dissolved in a PB-selective solvent, n-tetradecane (C14). At low temperatures, the PS-PB/C14 solutions contained micelles with PS cores and PB corona and exhibited plasticity and nonlinear dynamic responses. These unique properties were attributed to a macrolattice of micelles, that was in turn formed as a compromise of contradicting thermodynamic requirement, an *osmotic* requirement of uniform PB concentration distribution in the PB/C14 corona phase and an *elastic* requirement of randomizing the PB block conformation. Effects of these requirements were observed also for dielectric relaxation of styrene-*cis*-isoprene (PS-PI) diblock copolymer lamellar systems in bulk states. The PI blocks having type-A dipoles exhibited dielectric relaxation that reflected their global motion, and this relaxation was highly retarded and broadened due to the osmotic and elastic requirements.

KEY WORDS: Block Copolymers Micelles/ Thermodynamic Confinement/ Macrolattice/ Plasticity/ Dielectric Relaxation/ Type-A Dipole

1. INTRODUCTION

Microdomain formation is the most prominent feature of block copolymer chains. In strongly segregated state, the copolymer chains exhibit a variety of domain morphology (sphere, cylinder, ordered bicontinuous double diamond, lamella) according to the block composition and/or volume ratio of the domains.[1-3] Such microdomains have a well known thermodynamic origin:[2-4] Strongly segregated block copolymers are subjected to an *osmotic* requirement of maintaining uniform segment distribution in each microdomain and an *interfacial* requirement of reducing contacts of chemically different blocks. These thermodynamic requirements constrain the block chain conformation and tend to decrease the conformational entropy. On the other hand, an *elastic* requirement always tends to randomize the conformation and increase this entropy. These contradicting requirements *thermodynamically confine* the block copolymer chain, and their balance determines the microdomain morphology.[2-4]

Such block copolymers exhibit unique dynamic properties that are not observed for homogeneous homopolymer systems. Those properties are obviously influenced by the microdomain structures and thus by the thermodynamic forces for domain formation. It is of our particular interest to examine how the thermodynamic forces affect the dynamic properties. From this point of view, we have studied rheology and structures of styrene-butadiene (PS-PB) diblock copolymers dissolved in a PB-selective solvent, n-tetradecane (C14).[5-9] We also studied dielectric properties of styrene-*cis*-isoprene (PS-PI) diblock copolymers in bulk

* 渡辺　宏: Division of Fundamental Material Property I, Institute for Chemical Research, Kyoto University, Uji, Kyoto 611, Japan

states.[9-11] Dipoles of the PI blocks parallel to the chain contour enabled us to dielectrically observe global motion of the PI block. This paper summarizes the results, placing emphasis on the thermodynamic effects commonly observed for the rheological and dielectric properties.

2. EXPERIMENTAL

Material: Anionically polymerized PS-PB and PS-PI diblock copolymers were used. Their characteristics are summarized in Table I.

Measurements: Rheological measurements were carried out on solutions of the PS-PB samples in a PB-selective solvent, n-tetradecane (C14).[5-9] At low temperatures, spherical micelles with PS cores and PB corona were formed in the solutions. Higher order structure of those micelles was elucidated from small angle x-ray scattering (SAXS) measurements.[5-9]

Dielectric measurements were carried out on the PS-PI samples in bulk states.[9,10] The samples were cast on an electrode from homogeneous toluene solutions and thoroughly dried, and PS/PI alternating lamellae essentially parallel to the electrode were formed. At temperatures well below the glass transition temperature T_g^{PS} of the PS blocks, time-temperature superposition was valid for the dielectric data and the shift factor was identical to that for homo-PI,[9,10] meaning that the PS block motion was frozen and the dielectric dispersions observed were due only to the motion of the PI blocks.

3. RESULTS AND DISCUSSION

3-1 Rheology and Structure of Micellar Solutions.

Plasticity of Micellar Solutions: Figure 1 shows steady flow behavior at various temperatures for a 20 wt% n-tetradecane (C14) solution of the PS-PB 16-36 copolymer. At low temperatures $T \leq 60°C$, the solution clearly exhibits plastic flow behavior that is never observed for usual homopolymer solutions. This unique feature, plasticity, disappears and the solution becomes a non-Newtonian viscous liquid as T is increased up to 70°C. At higher $T \geq 95°C$, the solution becomes a Newtonian liquid with low viscosity.

The PS-PB 16-36 copolymer chains in the PB-selective solvent, C14, form spherical micelles with PS cores and PB corona at low T. However, this micellar structure itself cannot provide plasticity to the solution, and we naturally expect a higher order structure of the micelles. This structure is identified in Figure 2 where SAXS profiles are compared for the 20 wt% PS-PB 16-36/C14 solution at various temperatures. The profiles were diagonally shifted for easy comparison.

As seen in Figure 2, the PS-PB/C14 solution at 25°C exhibits the first, second, and third order scattering peaks due to inter-micellar interference at angles of 11.9, 16.5, and 20.8 min, respectively. These peaks indicate that the micelles are arranged on a so-called *macrolattice* having a long-range order.[5,7-9] (Detailed analysis of the SAXS data suggested that the macrolattice was most likely a simple-cubic lattice, or a body-centered cubic lattice, but not a face-centered cubic lattice.[12]) A lattice spacing (=450Å) evaluated from the peak angles is smaller than the micelles size (= 620Å),[5,12] indicating a rather deep overlapping of the corona PB blocks of neighboring micelles. Up to 60°C the SAXS profile remains essentially the same, and the long-range order of the macrolattice is preserved. At 70°C the higher order peaks

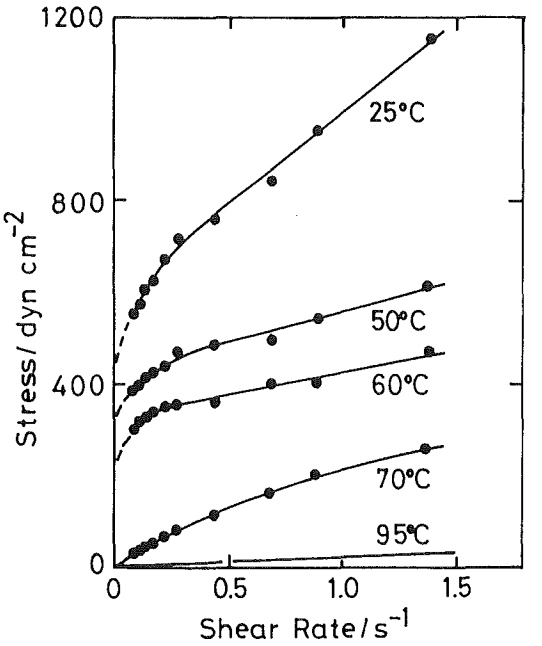

Fig. 1. Steady flow behavior of the 20 wt% PS-PB 16-36/C14 solution examined in a Couette geometry. Dashed curves indicate Bingham flow curves for the solution with the yield values and plastic viscosities evaluated in a cone-and-plate geometry.

disappear and the first order peak is broadened, indicating that the macrolattice is disordered but the micelles themselves are still preserved. Finally, at higher temperatures ($\geq$100°C) the micelles disappear due to mixing of PS and PB blocks, as noted from the disappearance of the first order peak. These structural changes well correspond to the rheological changes seen in Figure 1, and the plasticity of the PS-PB/C14 solution at low T is attributed to the macrolattice of micelles: As seen later in Figure 3, the macrolattice elastically deforms for stresses σ being smaller than the lattice strength ($\cong$ yield value σ_y) while it flows without disrupting micelles for $\sigma > \sigma_y$.

Corresponding to the steady plastic flow behavior (Figure 1), PS-PB/C14 micellar solutions exhibited unique dynamic responses against oscillatory strain. As an example, Figure 3 shows Lissajous patterns ($\omega = 0.0524$ s^{-1}) obtained at 25°C for the 20 wt% PS-PB 16-36/C14 solution containing a stable macrolattice (cf. Figure 2). As seen in Figure 3a, the solution exhibits a rectilinear pattern against a small amplitude strain that induces $\sigma < \sigma_y$ ($\cong$400 dyn cm^{-2}; cf. Figure 1). This pattern was independent of ω (unless ω was very high),[5,7-9] indicating the elastic response of the macrolattice before yielding. On the other hand, for a large amplitude strain inducing $\sigma \geq \sigma_y$, the solution exhibits a lozenge-shaped pattern (Figure 3b). A similar pattern was observed also for an aqueous dispersion of charged PS latexes that formed a lattice due to electrostatic repulsion.[5] Thus, lattice forming fluids commonly exhibit nonlinear responses demonstrated in Figure 3.

The lozenge-shaped Lissajous pattern is phenomenologically related to the plasticity of

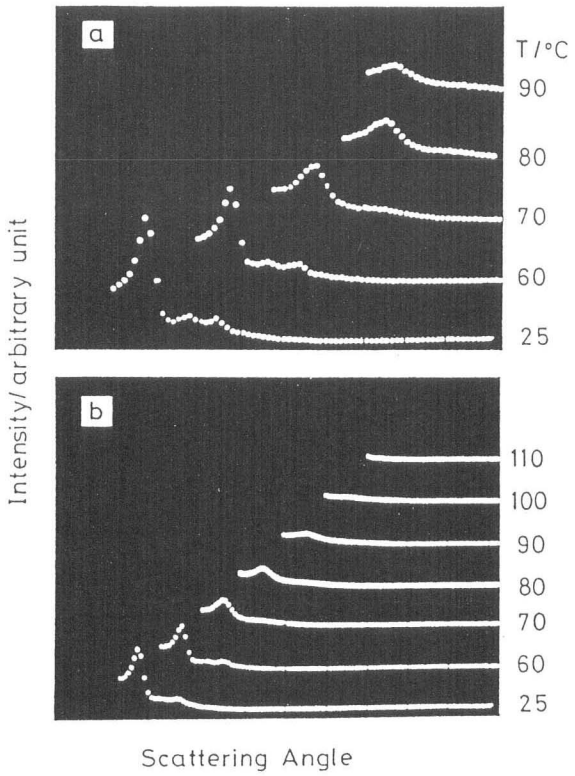

Fig. 2. SAXS profiles of the 20 wt% PS-PB 16-36/C14 solution at various T as indicated. Each channel corresponds to 0.7 min of arc, and the origins of the profiles are shifted right and upward for easy comparison. No desmearing correction was made for the data.

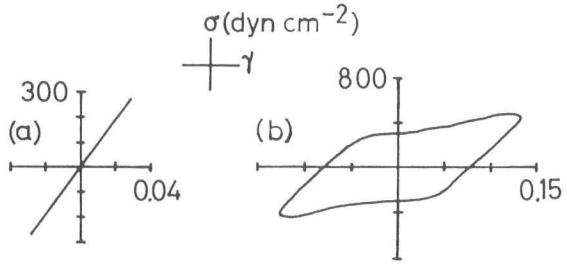

Fig. 3. Lissajous patterns at $\omega = 0.0524\ s^{-1}$ for the 20 wt% PS-PB 16-36/C14 solution at 25°C. Note the difference in the strain amplitudes in parts a and b.

the system: In each cycle of oscillation, the elastic deformation followed by plastic flow is repeated twice in opposite direction to give that pattern.[5] The lozenge-shaped pattern should be also related to the lattice structure itself. From this point of view, we here examine a lattice model developed by Doi, Harden, and Ohta.[13] Their results can be summarized as follows: For a lattice system composed of N lattice layers, the stress $\sigma(t)$ is considered to be uniform throughout the system. Then, $\sigma(t)$ is related to a local strain of k-th lattice layer γ_k (k = 1,2,..,N) as

$$\sigma(t) = G_0 \sin[\gamma_k(t)] + \int_{-\infty}^{t} dt' \, G_1 \exp[-(t-t')/\tau] \frac{d\gamma_k(t')}{dt'} \quad (1)$$

Here, the first term indicates the stress due to a thermodynamic potential for the lattice formation, and the second term, a contribution of some relaxation mechanism (like domain deformation) having a characteristic time τ. Differing from the stress, the strain is not necessarily uniform in the system. Then, the macroscopic strain γ is given as an average of γ_k,

$$\gamma = \frac{1}{N} \sum_{k=1}^{N} \gamma_k \quad (2)$$

Equations 1 and 2 provide a constitutive equation that describes rheological properties of the model lattice. (Modification of the potential and relaxation terms in eq 1 does not qualitatively change the following model prediction.[13])

For small γ, eqs 1 and 2 have a trivial solution, $\gamma_k = \gamma$ (k =1,2,..N). This solution corresponds to uniform deformation in the lattice and leads to a solid-like linear viscoelastic response.[13] Specifically, at long time scales (at low ω), the relaxation term in eq 1 vanishes and the elastic response with the equilibrium modulus G_0 is obtained. On the other hand, for large γ, the solution of eqs 1 and 2 is bifurcated and the trivial solution becomes unstable if the lattice includes even a tiny structural imperfection (that always exists in real lattice systems).[13] For this case, eqs 1 and 2 have a stable solution representing a *lattice plane slippage*, $\gamma_k \neq \gamma$, and this solution leads to plastic steady flow behavior as well as nonlinear dynamic responses characterized with a lozenge-shaped Lissajous pattern.[13] Thus, the Doi-Harden-Ohta model qualitatively explains all characteristic features of the PS-PB/C14 micellar solution (Figures 1 and 3), suggesting that the plasticity of the solution is attributed to the slippage of the macrolattice planes.

Here, we would like to add a comment on structure-rheology relationship for lamellar block copolymer systems.[14,15] Those systems exhibit very slow power-law type stress relaxation,[14,15] as is similar to the elastic behavior of the PS-PB/C14 micellar systems *in a sense that the terminal relaxation is not observed in usual time scales.* However, the structural origin of the stress at long time scales is not the same for the two systems. The stress is generated whenever the macroscopic strain distorts the domain alignment. From this point of view, the stress for the lamellar systems at long time scales is attributed to defects of the lamellar alignment.[14,15] In fact, the stress is decreased when the lamellae are highly aligned to have less defects and the resulting *one-dimensional* long-range order of the lamellar alignment is not distorted by the applied strain.[14,15] On the other hand, the elastic stress of the micellar systems is due to deformation of the macrolattice: Any strain distorts the *three-dimensional* (cubic) order of the macrolattice and thus generates a restoring force even if no defect exists. Thus, the difference in rheological properties of the lamellar and micellar systems is related to the difference in the spatial symmetry of their domain alignment. (However, some effect of

defects exists also for the elasticity of the macrolattice, as discussed later in Figure 5.)

Driving Force for Macrolattice Formation: The macrolattice of PS-PB micelles is formed most likely due to a balance of the thermodynamic requirements explained earlier. In the micellar solution examined in Figures 1 and 2, the PS-cores are glassy at low T. For such cases, the number of PS-PB contacts should be essentially the same for the two cases of randomly dispersed and regularly arranged micelles, and the interfacial requirement would have no effect for the macrolattice formation. However, a balance of the osmotic and elastic requirements should still take place for the PB blocks that are tethered on the rigid PS cores. The macrolattice would have been formed so that the PB concentration (C_{PB}) distribution in the PB/C14 corona phase became as uniform as possible while the PB block conformation became as random as possible.

This hypothesis was critically tested in two ways. In the first test, an overlapping concentration of micelles (C*) in PS-PB/C14 solutions was compared with the rheological transition concentration (C_R*) above which the plasticity due to macrolattice emerges.[7,8] For the PS-PB samples listed in Table I, C_R* and C* are summarized in Table II. As seen there, C_R* is considerably close to C* and both C_R* and C* decrease with increasing PB block molecular weight. This result suggests that the macrolattice is formed at around C* where the osmotic requirement on the PB blocks becomes enhanced, supporting the above hypothesis.

In the second critical test, rheological behavior was examined on ternary systems composed of the PS-PB 16-36 copolymer, C14, and homo-PB (hPB) with M = 2000.[6] Figure 4 shows their steady flow behavior at 25°C. In the systems examined, the PS-PB content was always 20 wt% and the hPB content w_{hPB} in the remaining 80 wt% was varied. The PS-PB copolymers always formed spherical micelles with the PS cores and PB-corona, and the hPB molecules were involved in the PB/C14 corona phase.

As seen in Figure 4, the yield stress decreases with increasing w_{hPB} and finally vanishes for w_{hPB} = 50 wt%. This result indicates that the hPB chains destroy the macrolattice, as

Table I. Characteristics of PS-PB and PS-PI samples.

Code[a]	$10^{-3}M_{PS}$	$10^{-3}M_{PD}$[b]	M_w/M_n
	PS-PB Diblock Copolymers		
PS-PB 16-36[c]	16	36	1.5
PS-PB 20-46	20	46	1.06
PS-PB 20-100	20	100	1.07
PS-PB 32-102	32	102	1.07
PS-PB 32-160	32	160	1.08
PS-PB 32-262	32	262	1.10
	PS-PI Diblock Copolymers		
PS-PI 5-5	5.3	4.6	1.05
PS-PI 13-10	12.5	9.5	1.06
PS-PI 42-43	41.5	42.5	1.07

a: code numbers indicate block molecular weights in unit of 1000.
b: polydiene block molecular weight; PD = PB or PI
c: Solprene 1205 (Phillips Co.)

Table II. Comparison of critical concentration C_R^* for plastic-to-viscous transition and micelle-overlapping concentration C^* for PS-PB/C14 solutions at 25°C.

Sample	C_R^* (wt%)	C^* (wt%)
PS-PB 16-36	9-10	6.8
PS-PB 20-46	6-7	3.8
PS-PB 20-100	2-3	2.5
PS-PB 32-102	3-4	2.3
PS-PB 32-160	1-2	2.2
PS-PB 32-262	1.2-1.5	1.6

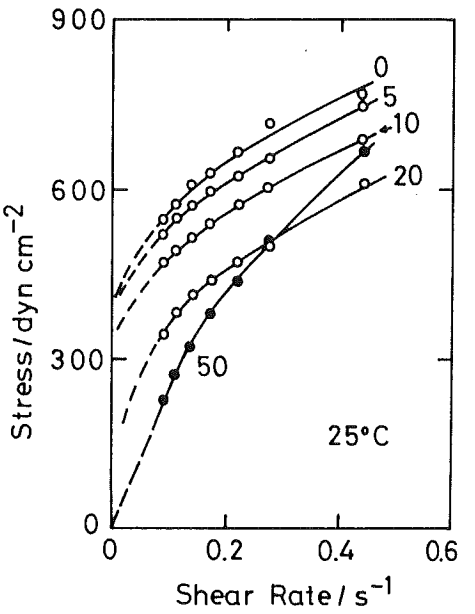

Fig. 4. Steady flow behavior of the PS-PB 16-36/hPB/C14 ternary systems at 25°C. The PS-PB content is 20 wt% for all systems, and the numbers in the figure indicate the hPB content w_{hPB} (in wt%) in the remaining 80 wt%.

also confirmed from SAXS measurements.[6] This effect of hPB supports the above hypothesis for macrolattice formation: A spatial variation of C_{PB} due to randomization of PB block conformation can be compensated by the hPB chains that have no tethered ends and can move in the PB/C14 corona phase without a large burden on their conformation. Thus, in the ternary systems with large w_{hPB}, the osmotic and elastic requirements are no longer contradicting for the PB blocks and no driving force for macrolattice formation emerges.

As demonstrated in the above critical tests, the micelles are arranged on the macrolattice so that the osmotic and elastic requirements for the corona PB blocks are compromised.

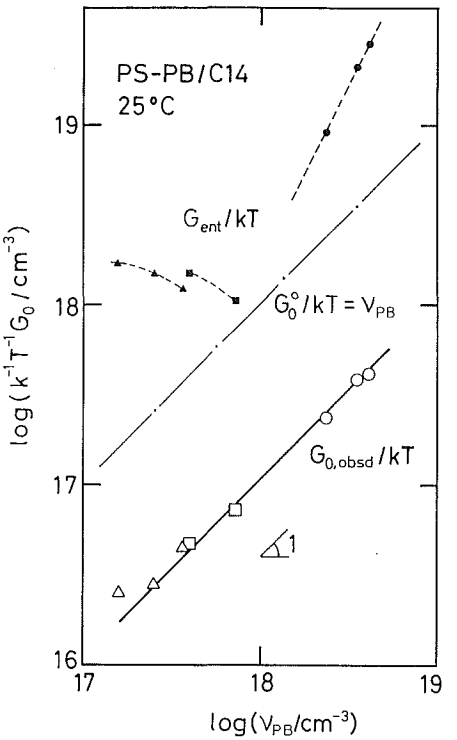

Fig. 5. Dependence of equilibrium modulus for PS-PB/C14 solutions at 25°C on number density of PB blocks. Rigid macrolattices of spherical micelles are formed in all solutions. Unfilled circles: data for 20, 30, and 35 wt% PS-PB 16-36/C14 solutions; Unfilled squares: data for 10 wt% C14 solutions of PS-PB 20-46 and 20-100; Unfilled triangles: data for 10 wt% C14 solutions of PS-PB 32-102, 32-162, and 32-262. Small filled symbols connected with the dashed curves indicate entanglement plateau moduli for the solutions, and the dash-dot line is the equilibrium modulus expected for a perfect macrolattice without defects.

Thus, the thermodynamic stability of the macrolattice is determined by those requirements. This stability is observed as the modulus G_0 of the PS-PB/C14 solutions at sufficiently low ω where the solutions exhibit elastic responses against small amplitude strain (cf. Figure 3a). Figure 5 shows dependence of G_0/kT at $\omega = 0.0136\ s^{-1}$ (kT = thermal energy) on the PB block number density ν_{PB} ($\propto C_{PB}/M_{PB}$) for C14 solutions of the PS-PB samples listed in Table I. The data for 20, 30, and 35 wt% PS-PB 16-36/C14 solutions are indicated with the unfilled circles, and those for 10 wt% C14 solutions of the other five PS-PB samples, with the unfilled squares and triangles. These concentrations are well above C_R^* (Table II) and the solutions contain rigid macrolattices.

Figure 5 clearly demonstrates differences between G_0 and the entanglement plateau modulus G_{ent} (small filled symbols): G_0 is significantly smaller than G_{ent}, meaning that G_0 shown here has no entanglement contribution and is regarded as the equilibrium modulus. In addition, G_0 is proportional to ν_{PB} irrespective of M_{PB}, while G_{ent} ($\propto C_{PB}^2$) depends on both ν_{PB}

and M_{PB}. The proportionality between G_0 and ν_{PB} indicates that each PB block works as an elastic strand to resist the small strain applied on the system. This result is in accordance with the feature of the driving force for macrolattice formation: In concentrated solutions examined in Figure 5, an osmotic compressibility is considerably small[16] so that the strain should hardly change the C_{PB}-distribution in the PB/C14 corona phase. Then, the strain is directly transmitted to PB block conformation and each PB block as a whole behaves as the elastic strand,[17] leading to the relation $G_0 \propto \nu_{PB}$.

In Figure 5, we also find a puzzling result. The observed G_0 is 10 times smaller than the equilibrium modulus expected for a perfect macrolattice without defects, $G_0^\circ = \nu_{PB}kT$ (dash-dot line). This result suggests that defects involved in actual macrolattices reduce the lattice rigidity. However, details of the reduction of rigidity due to defects are not yet clarified, and a further study is desired.

3-2 Dielectric Relaxation of Block Copolymer Lamellar Systems.

The previous section examined thermodynamic effects on very slow dynamics of strongly segregated block copolymers through rheological tests. It is also interesting to study the effects on faster dynamics. For this purpose, we here examine dielectric relaxation of styrene-*cis*-isoprene (PS-PI) diblock copolymers at time scales covering both segmental and global motion of the PI blocks.

PI chains have so-called *type-A dipoles*[18] parallel along their contour, so that their global motion (end-to-end vector fluctuation) induces prominent dielectric relaxation at long time scales.[9-11,19,20] In addition, PI chains also have type-B dipoles[18] perpendicular to the contour and exhibit fast dielectric relaxation corresponding to their segmental motion.[9-11,19,20] Thus, at T well above T_g^{PI} of the PI blocks but well below T_g^{PS} of the PS blocks, PS motion is frozen and we can clearly observe the segmental and global motion of the PI blocks through the dielectric behavior of the PS-PI copolymers.

Figure 6 shows dielectric loss (ε'') curves at 0°C for the bulk PS-PI copolymers listed in Table I (symbols). PS/PI lamellae essentially parallel to the electrodes of a dielectric cell are formed in the system, and the dielectric dispersions seen here are attributed to motion of the PI blocks tethered on glassy PS domains. For comparison, ε'' data for precursor homo-PI (hPI) chains with molecular weights being identical to M_{PI} of the PI blocks are indicated with the dotted, solid, and dashed curves. Both PI block and hPI exhibit two distinct relaxation processes: The M_{PI}-independent relaxation at high ω is induced by the segmental motion, while the M_{PI}-dependent relaxation at low ω is due to the global motion.

The PI blocks in the lamellae should be thermodynamically confined by the osmotic and elastic requirements explained in the previous section, while the hPB chains are not. Nevertheless, Figure 6 indicates that the shape and location of the ε'' curve at high-ω are nearly the same for the PI block and hPI. (The difference in the ε'' peak height is mainly due to the difference of the PI content in the system.) This result suggests that the segmental motion of the PI blocks is hardly affected by the thermodynamic confinement.

On the other hand, significant differences are found in Figure 6 for the low-ω relaxation of the PI blocks and corresponding hPI: For hPI the terminal relaxation characterized by a relation, $\varepsilon'' \propto \omega$, is observed as soon as ω is decreased below the ε''-peak frequency ω_p, while for the PI block ε'' is almost proportional to $\omega^{1/2-1/3}$ and terminal relaxation is not

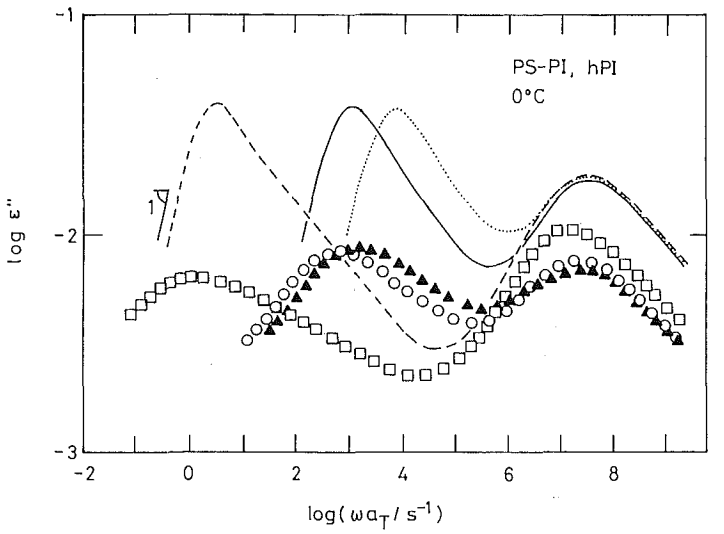

Fig. 6. Dielectric loss (ε '') curves at 0°C for the PS-PI 5-5 (triangles), 13-10 (circles), and 42-43 (squares) samples in bulk state. For the PI blocks of these copolymers, ε '' data of corresponding hPI precursors are shown with the dotted, solid, and dashed curves, respectively. Small corrections for segmental friction were made for the shortest PI block and hPI (triangles and dotted curve).

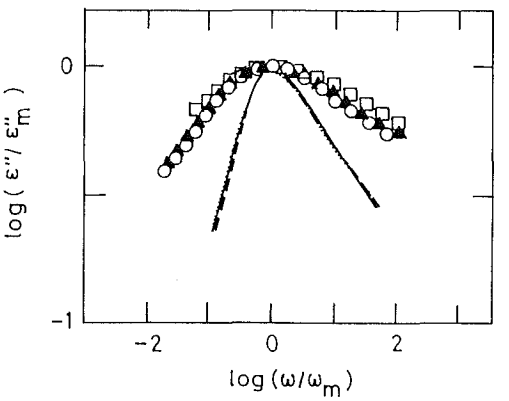

Fig. 7. Comparison of shape of the ε '' curve *at low* ω for the PS-PI and hPI samples examined in Figure 6. The sense of the symbols is the same as in Figure 6. Note that the shape of the curve reflects dielectric relaxation mode distribution.

attained even at $\omega \ll \omega_p$. (Note that the ε '' peak of the PI block does not correspond to the terminal relaxation.) Thus, the low-ω relaxation due to end-to-end vector fluctuation is much slower and broader for the PI block than for hPI having the same M_{PI}.

Figure 7 compares the shape (ω dependence) of the ε '' curves at low ω for the PI

blocks and hPI examined in Figure 6. For easy comparison, the curves are reduced at their peaks. The shape of the ε'' curve reflects the dielectric mode distribution. Figure 7 indicates that the mode distribution of hPI is quite insensitive to M_{PI} at long time scales (cf. dotted, solid, and dashed curves), as also found in a previous study.[20] More importantly, almost M_{PI}-independent mode distribution is observed also for the PI blocks (symbols).

The shortest PI block examined in Figures 6 and 7 has M_{PI} well below M_e ($=10\times10^3$; entanglement molecular weight[21]) and is in the non-entangled state, while the other two PI blocks (with $M_{PI} \cong M_e$ and $4M_e$) are entangled. Nevertheless, the unentangled and entangled PI blocks exhibit essentially the same relaxation mode distribution (cf. Figure 7). In addition, at low-ω relative location of the ε'' curves for the PI block and corresponding hPI is insensitive to M_{PI}, as seen in Figure 6. These results strongly suggest that the broad and retarded dielectric relaxation of the PI blocks is not due to entanglements but is essentially due to the thermodynamic requirements that constrain the global motion of the PI block.

The osmotic requirement is extremely strong for the PI blocks in bulk state, so that the motion of the PI blocks should be highly cooperative to maintain the uniform PI segment distribution in the PI lamellae. During this cooperative motion, the PI blocks having tethered ends should violate the elastic requirement and pay some entropic penalty to take distorted conformations. These cooperativity and penalty most likely lead to the very slow and broad relaxation behavior of the PI blocks. The relaxation of the PI blocks looks similar to that of entangled star chains[22] in a sense that the retardation takes place due to an entropic penalty, although the penalty emerges from the thermodynamic confinement for the former but from the entanglement effect for the latter.

From the above argument, we expect that the dielectric behavior of PS-PI copolymers becomes closer to that of hPI chains when a PI-selective solvent is added, because the solvent increases the osmotic compressibility and weaken the above requirement of cooperativity. This expectation was confirmed experimentally.[11] Another consequence of the above argument is for the M_{PI} dependence of the longest relaxation time τ_1 of the PI blocks. Although τ_1 were too long to be determined in our experiments, the similarity between the PI blocks and entangled star chains suggests τ_1 for the PI blocks to increase exponentially with M_{PI}.[23] A test for this expectation is interesting future work.

4. CONCLUDING REMARKS

We have found that PS-PB/C14 micellar solutions exhibit plasticity and nonlinear dynamic responses that are attributed to the macrolattice of micelles. The macrolattice is formed so that the osmotic and elastic requirements are compromised. Thus, the plasticity and nonlinearity of the micellar solutions are a rheologically observed thermodynamic effect. The effect was also observed for the slow dielectric relaxation of PS-PI diblock copolymers that reflects global motion of the PI blocks. The relaxation is strongly retarded and broadened due to the osmotic and elastic requirements on the PI blocks. Thus, the slow relaxation of the PI blocks and the unique rheology of the micellar solutions commonly have a thermodynamic origin. It is of particular interest to interrelate other characteristic properties of block copolymers (like enhanced adhesion[9,24]) under the concept of thermodynamic confinement.

REFERENCES

(1) See, for example, G. E. Molau, in "Block Copolymers", S. L. Aggarwal Ed., Plenum, New York, 1970.
(2) T. Hashimoto, in "Polymer Alloy", 1st Ed., T. Kotaka, F. Ide, and K. Ogino Eds., Kagaku Dojin, Tokyo, 1981.
(3) F. S. Bates and G. H. Fredrickson, *Ann. Rev. Phys. Chem.*, **41**, 525 (1990).
(4) E. Helfand and Z. R. Wasserman, *Macromolecules*, **9**, 829 (1976); *ibid.*, **11**, 960 (1978).
(5) H. Watanabe, T. Kotaka, T. Hashimoto, M. Shibayama, and H. Kawai, *J. Rheol.*, **26**, 153 (1982).
(6) H. Watanabe and T. Kotaka, *J. Rheol.*, **27**, 223 (1983).
(7) H. Watanabe and T. Kotaka, *Polym. Eng. Rev.*, **4**, 73 (1984).
(8) T. Kotaka and H. Watanabe, in "Current Topics in Polymer Science (Vol. II)", R. M. Ottenbrite, L. A. Utracki, and S. Inoue Eds., Hanser Publishers, New York, 1987.
(9) H. Watanabe and T. Kotaka, in "Ordering in Macromolecular Systems", A. Teramoto, M. Kobayashi, and T. Norisuye Eds., Springer, Berlin, 1994.
(10) M. L. Yao, H. Watanabe, K. Adachi, and T. Kotaka, *Macromolecules*, **24**, 2955 (1991).
(11) M. L. Yao, H. Watanabe, K. Adachi, and T. Kotaka, *Macromolecules*, **24**, 6175 (1991).
(12) M. Shibayama, T. Hashimoto, and H. Kawai, *Macromolecules*, **16**, 16 (1983).
(13) M. Doi, J. L. Harden, and T. Ohta, *Macromolecules*, **26**, 4935 (1993).
(14) R. G. Larson, K. I. Winey, S. S. Patel, H. Watanabe, and R. Bruinsma, *Rheol. Acta*, **32**, 245 (1993).
(15) K. A. Koppi, M. Tirrell, F. S. Bates, K. Almadal, and R. Colby, *J. Phys. II (Paris)*, **2**, 1941 (1993).
(16) I. Noda, N. Kato, T. Kitano, and M. Nagasawa, *Macromolecules*, **14**, 668 (1981).
(17) T. Hashimoto, M. Shibayama, H. Kawai, H. Watanabe, and T. Kotaka, *Macromolecules*, **16**, 361 (1983).
(18) W. H. Stockmayer, *Pure Appl. Chem.*, **15**, 539 (1969).
(19) Y. Imanishi, K. Adachi, and T. Kotaka, *J. Chem. Phys.*, **89**, 7585 (1988).
(20) H. Watanabe, M. Yamazaki, H. Yoshida, K. Adachi, and T. Kotaka, *Macromolecules*, **24**, 5365 (1991).
(21) J. D. Ferry, "Viscoelastic Properties of Polymers", 3rd ed., Wiley, New York, 1980.
(22) M. Doi and S. F. Edwards, "The Theory of Polymer Dynamics", Clarendon: Oxford, 1986.
(23) T. A. Witten, L. Leibler, and P. A. Pincus, *Macromolecules*, **23**, 824 (1990).
(24) H. Watanabe and M. Tirrell, *Macromolecules*, **26**, 6455 (1993).